Bull. Inst. Chem. Res., Kyoto Univ., Vol. 72, No. 2, 1994

Amorphous-forming Regions of RF-Sputtered Films in the B_2O_3-Na_2O System

Rikuo OTA*, Takasi WAKASUGI*,
Yosiyuki NOZAWA and Jiro FUKUNAGA*

Received May 19, 1994

The variation of amorphous regions of the sputtered films in the B_2O_3-Na_2O system with sputtering power, sputtering time and substrate temperature has been investigated. The amorphous regions are $B_2O_3=0\sim78.8$ mol% ranges in the B_2O_3-Na_2O system under a sputtering power 100 W, sputtering time 20 h and substrate temperature 90°C. Decreasing sputtering power from 100 W to 50 W, decreasing sputtering time from 20 h to 5 h expanded amorphous regions and increasing substrate temperature from 90°C to 250°C reduced the amorphous regions. These results were compared with the variation of the critical cooling rate for glass formation from the melt of the system.

KEY WORDS : Amouphous-Forming Region/ RF-Sputtering/ Film/ Critical Cooling Rate/ B_2O_3-Na_2O System

1. INTRODUCTION

It has been well recognized that amorphous substances are produced in various methods including sol-gel method, sputtering technique and CVD method other than the melt-quenching method. Boron trioxide (CVD)[1] and silicon dioxide (sol-gel, sputtering and CVD) are the examples for such amorphous materials. Alumina is an example that can be transformed into an amorphous state by sputtering[2] and sol-gel methods,[3] but amorphous alumina has never been obtained by melt-quenching method despite the great effort utilizing the rapid quenching technique. MgO and CaO are the examples that can not be transformed into an amorphous state even by sputtering technique.[4] In the present study amorphous regions and the thermal stability of the sputtered films are compared with those of the melt-quenched glasses in the B_2O_3-Na_2O system.

2. EXPERIMENTAL

2.1 Sputtering condition

Sputtering apparatus was ULVAC SH-100B model by NIHON SHINNKU Co.Ltd. Chamber pressure was maintained at $0.6\sim0.7$ Pa level with a sputtering gas of Ar and O_2 mixture of $Ar/O_2=3/1$. The sputtering power was varied, 50 W or 100 W, in order to see the effect of power on the variation in amorphous regions. The sputtering condition is shown in Table 1. Substrates were selected from commercial glass of soda-lime-silica composition or

* 大田陸夫, 若杉 隆, 野沢善幸, 福永二郎 : Department of Chemistry and Materials Technology, Kyoto Institute of Technology, Matsugasaki, Sakyo-ku, Kyoto 606, Japan.

Table 1. Sputtering condition.

Sputtering power	50 W, 100 W
Sputtering gas	$Ar/O_2=3/1$
Sputtering pressure	0.6~0.7 Pa
Sputtering time	1~20 h
Targets	B_2O_3-Na_2O glass or crystal
	SiO_2 glass for protective sputtering
Substrates	Al_2O_3 for chemical analysis
	Soda-lime-silica glass for XRD and film thickness measurement
Substrate temperatures	90, 250°C

alumina according to the experimental objectives. Alumina substrate was used for the composition analysis of the B_2O_3-Na_2O films. Commercial soda-lime-silica glass substrate was utilized for the determination of amorphous regions and measurements of film thickness in order to evaluate the deposition rate. Substrate temperature was 90°C or 250°C. The sputtering power was 50 W or 100 W and sputtering time ranged from 5 to 20 h.

2.2 Preparation of targets

Targets in the form of disk 4 mm thick and 60 mm in diameter were prepared by quenching the B_2O_3-Na_2O melts of given compositions fused at 1,000°C for 1h. Silica glass plate or silica glass powder was used as target material for protective sputtering (see 2.3) over the sputtered films of hygroscopic, B_2O_3 rich or Na_2O rich compositions.

2.3 Protective sputtering

Hydration takes place immediately in the ambient atmosphere at the film surface of pure B_2O_3 or Na_2O rich (more than 50 mol% Na_2O) compositions. To protect the sputtered films from hydration, SiO_2 film of 1 μm was deposited over the B_2O_3-Na_2O films under the condition of sputtering power 50 W and sputtering time 25 h. It was proved that X-ray diffraction can detect crystalline phases in the film sample below the protective SiO_2 film. A possible disturbing effect such as diffusion of silica into the underlying film or reaction of silica with the film, was examined by EMA line probing along the cross section of the protectively sputtered sample. No hazardous result was perceived under the present condition.

2.4 Compositional analysis of sputtered films by WDX analysis

Chemical composition of the sputtered films was analyzed by use of WDX (X-650 model by HITACHI Co. Ltd.) using melt-quenched B_2O_3-Na_2O glasses as the reference. The concentration of B_2O_3 and Na_2O components were determined by volumetric and flame photometric method, respectively.

2.5 Amorphous regions and crystallization behavior of the sputtered films

The determination of amorphous regions was made by the X-ray diffraction method.

3. RESULTS AND DISCUSSION

3.1 Chemical analysis of sputtered films

Figure 1 indicates the chemical composition (Na_2O content) by WDX analysis of the B_2O_3-Na_2O films under different power 50 W or 100 W and sputtering time 1~5 h. The Na_2O

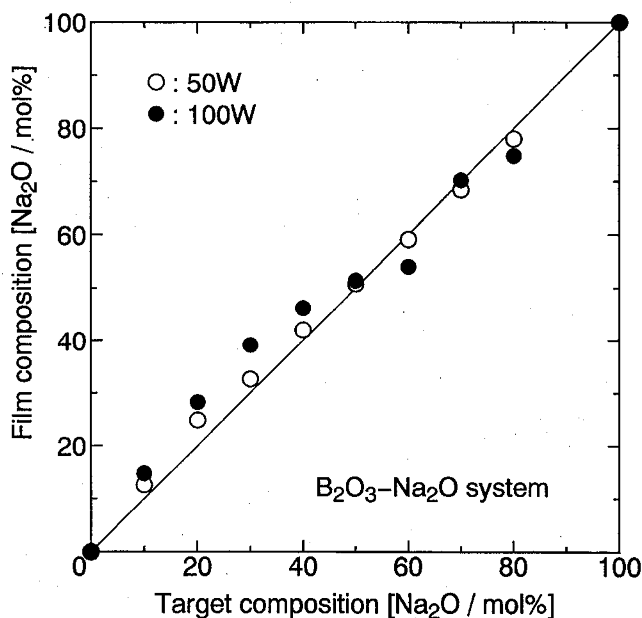

Fig. 1. Comparison of the film compositions (Na_2O content for example) with the target compositions in the B_2O_3-Na_2O system under the sputtering power 50 W (○) and 100 W (●).

content in sputtered films tend to be rich compared with that in the target for the $Na_2O=0\sim50$ mol% range. Maximum compositional deviation between the targets and the sputtered films amounts to 9% with sputtering power 100 W and to 5% with sputtering power 50 W. The fact that no deviation is observed at $Na_2O=50$ mol% suggests that particle with composition of the ratio B_2O_3 : $Na_2O=1:1$ is preferentially formed by sputtering process. According to the reports[5~7] MBO_2 composition (M=Li, Na, K, Rb) exhibits the highest vapor pressure among the alkali borate melts.

3.2 Deposition rate in the B_2O_3-Na_2O system

The average deposition rate was calculated from the film thickness and the sputtering time. The deposition rate for B_2O_3-Na_2O system is shown in Fig. 2. Figure 2 indicates a maximum deposition rate observed at $Na_2O=50$ mol% composition. The maximum of deposition rate at $Na_2O=50$ mol% can be ascribed to the high vapor pressure of the MBO_2 species as mentioned above.[5~7] As the sputtering power is doubled, from 50 W to 100 W, deposition rate increases nearly 3 times as much for all compositions.

3.3 Amorphous regions determined by X-ray diffraction

(i) Effect of protective SiO_2 sputtering against hydration

X-ray diffraction patterns of the as-deposited film (without protective SiO_2 sputtering) in the B_2O_3-Na_2O system on the commercial glass substrate are illustrated in Fig. 3. Precipitated phases are hydrated H_3BO_3 crystal at $Na_2O=0$ mol% composition, $B_2O_3{\cdot}Na_2O{\cdot}H_2O$ crystal at $Na_2O=46.2\sim78.8$ mol% compositions and sodium carbonate $NaCO_3$ at $Na_2O>78.8$ mol% composition.

It was speculated that the hydrated crystalline phases H_3BO_3 and $B_2O_3{\cdot}Na_2O{\cdot}H_2O$ had

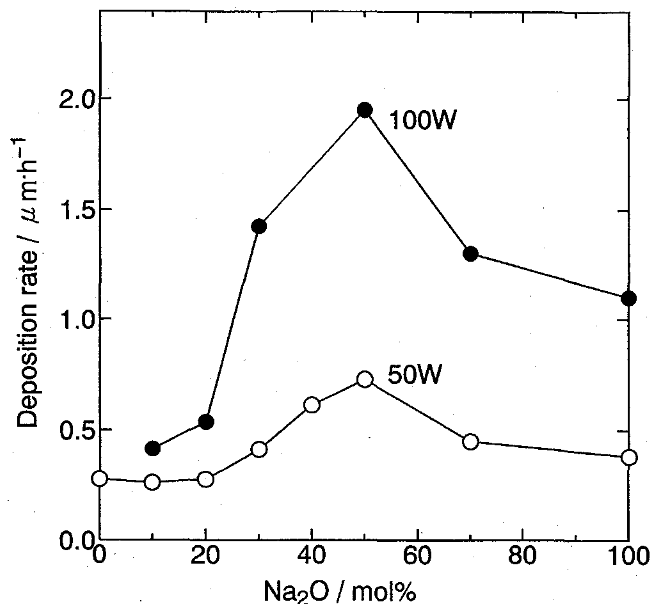

Fig. 2. Deposition rate of the B_2O_3-Na_2O system under sputtering power 50 W (○) and 100 W (●).

come from the hydration of the sputtered films during the XRD experiments in the humid circumstance. The hydration of B_2O_3 film was confirmed by measuring the growth of hydrated H_3BO_3 crystal by X-ray diffraction as a function of exposing time.

Fig. 4 indicates the increase of the X-ray diffraction intensity due to the formation of H_3BO_3 crystals when as-deposited B_2O_3 film is exposed to humid air. Hydration of B_2O_3 film becomes apparent after 6 min and the growth of the hydrated H_3BO_3 layer with time is clearly demonstrated. It is also shown that by a protective SiO_2 sputtering (film thickness 1 μm) over as-deposited B_2O_3 film under the sputtering power 100 W and substrate temperature 90°C, no hydration occurs in the humid atmosphere even after 20 min.

Figure 5 shows the X-ray diffraction of the protectively sputtered B_2O_3-Na_2O films. As compared with the non-protective sputtering (Fig. 3), hydrated compounds (H_3BO_3 and $B_2O_3 \cdot Na_2O \cdot H_2O$) did not precipitate. However, $NaCO_3$ was still observed in the Na_2O= 90~100 mol% compositions. With protective SiO_2 sputtering amorphous region was in the range of Na_2O=0~78.8 mol%. Ota and Soga[8] observed that substantial amount of undecomposed $NaCO_3$ is retained in the Na_2O rich borate melts even after a long heating at 1,000°C or higher temperatures. Crystalline $NaCO_3$ presumably came from undecomposed sodium carbonate retained in the target. The effect of protective SiO_2 sputtering against hydration on the change of amorphous region is shown in Fig. 6.

(ii) Effect of substrate temperature and sputtering power

Ota *et al.*[3] observed in the SiO_2-MgO system that the amorphous region in the sputtered films decreases with increasing sputtering power and increasing sputtering time and increasing substrate temperature. So it was anticipated that the amorphous region should decrease in the B_2O_3-Na_2O system as the substrate temperature increases.

Figure 7 indicates the X-ray diffraction patterns of the protectively sputtered films in the

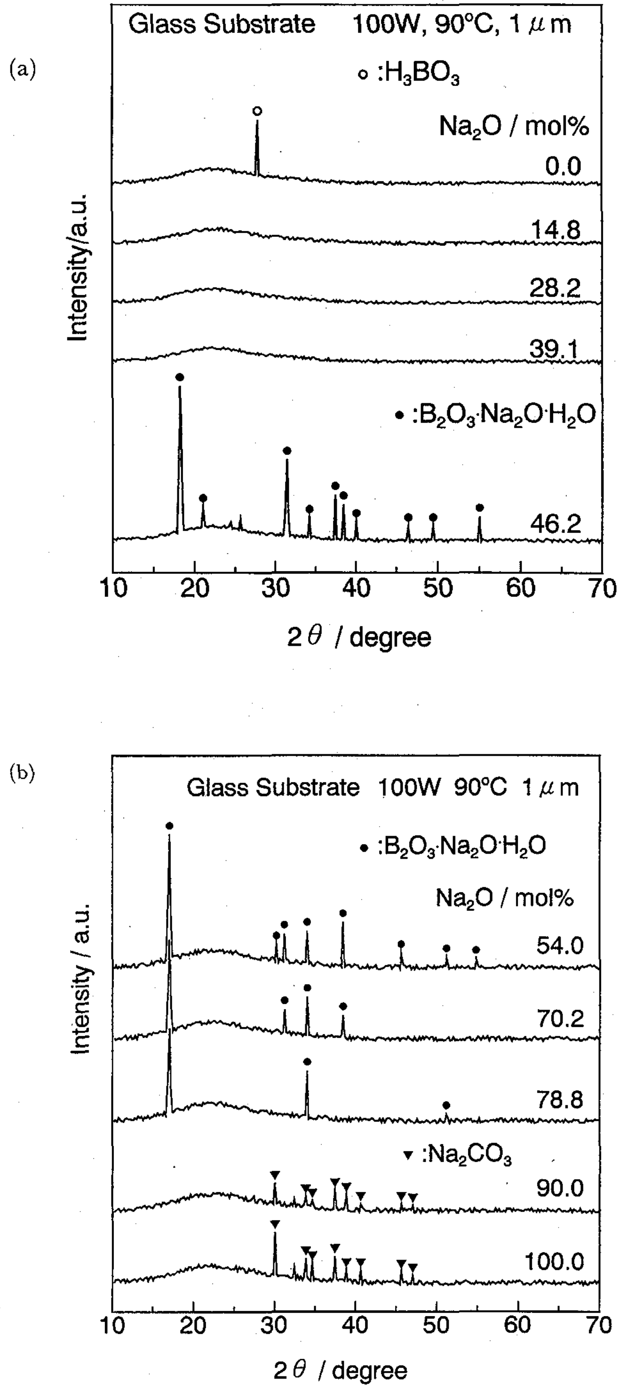

Fig. 3. X-ray diffraction patterns of as-deosited films 1 μm thick in the B_2O_3-Na_2O system sputtered over the soda-lime-silica gass substrate (without protective SiO_2 sputtering) under the sputtering power 100 W and substrate temperature 90°C.

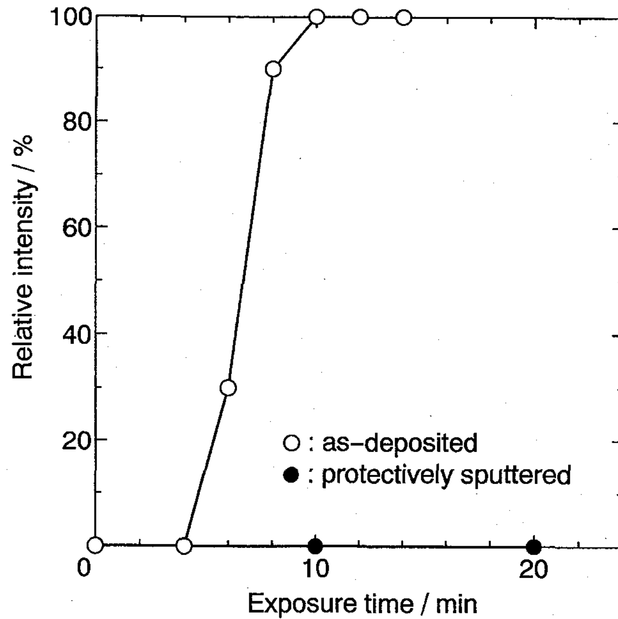

Fig. 4. Change of the X-ray diffraction intensity due to H_3BO_3 formation plotted against air-to-sample exposing time with (●) or without (○) protective SiO_2 sputtering of as-deposited B_2O_3 film.

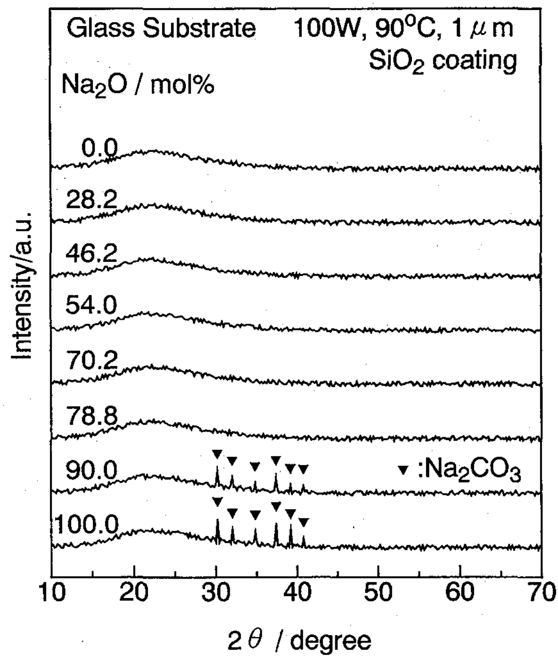

Fig. 5. X-ray diffraction patterns of protectively sputtered films in the B_2O_3-Na_2O system on the soda-lime-silica glass substrate under the sputtering power 100 W and substrate temperature 90°C.

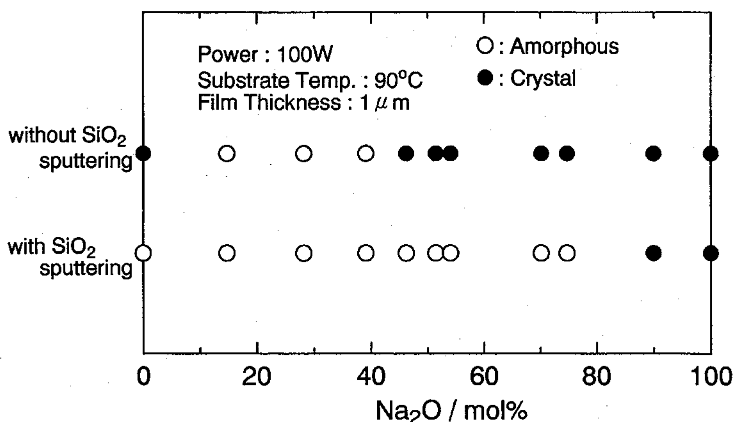

Fig. 6. Comparison of amorphous region of sputtered films in the B_2O_3-Na_2O system on the glass substrate with or without SiO_2 protective sputtering under the condition of sputtering power 100 W and substarte temperature 90°C.

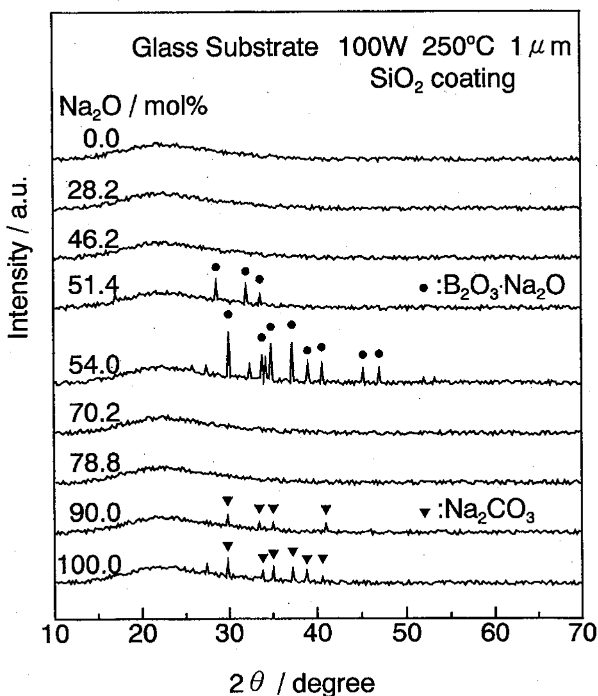

Fig. 7. X-ray diffraction patterns of protectively sputtered films in the B_2O_3-Na_2O system on the soda-lime-silica glass substrate under the sputtering power 100 W and substrate temperature 250°C.

B_2O_3-Na_2O system with substrate temperature 250°C, and sputtering power 100W. Crystalline $B_2O_3 \cdot Na_2O$ precipitated in the Na_2O=51.4~54 mol% composition range and $NaCO_3$ precipitated in the Na_2O=90~100 mol% compositions. Under this condition amorphous

regions are in fact Na_2O=0~46.2 mol% and 70.2~78.8 mol% composition ranges.

Figure 8a shows the effect of substrate temperature. The amorphous regions are compared in the protectively sputtered B_2O_3-Na_2O films prepared under different substrate temperature 90 or 250°C and sputtering power 100 W. Figure 8b shows the effect of sputtering power. The amorphous region of the protectively sputtered B_2O_3-Na_2O films increases with decreasing sputtering power from 100 W to 50 W under substrate temperature 250°C. The crystal region observed at the Na_2O=51.4~54 mol% composition range under the sputtering power 100 W disappeared and the amorphous region was extended to Na_2O=0~78.8 mol% range, which is the same amorphous limit observed under substrate temperature 90°C and sputtering power 100 W (Fig. 8a).

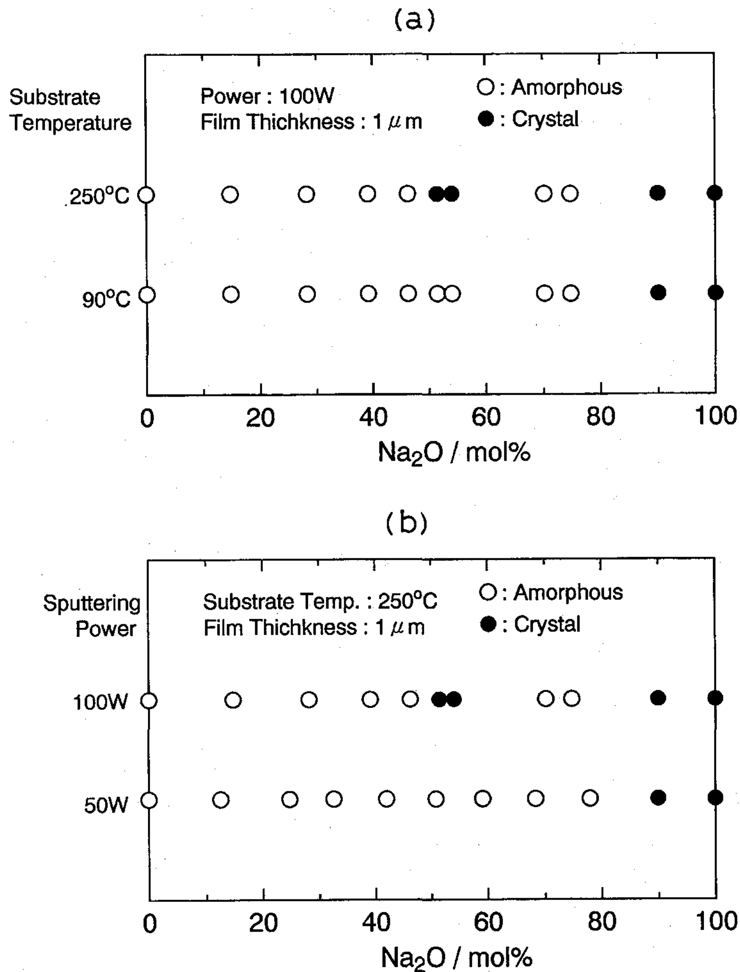

Fig. 8. Comparisons of amorphous regions of the protectively sputtered B_2O_3-Na_2O films under the sputtering power 100 W, sputtering time 20 h and substrate temperature 90°C and 250°C (a), and under sputtering power 100 W and 50 W, sputtering time 20 h and substrate temperature 250°C (b).

3.4 Comparison of amorphous regions by the sputtering and the melt-quenched method

Sputtering method may be regarded as a modified melt-quenching method wherein sputtered molecules (ions) solidify on the substrate via quasi-liquid phase with estimated quenching rate $>10^{12}$ °C/s.[9] So the amorphous regions in the sputtering and melt-quenching methods may show a similarity. Figure 9 represents the glass-forming regions obtained under various cooling rates in the B_2O_3-Na_2O system.[10,11] It is clear from Fig. 8 and Fig. 9 that apparent similarity is seen between the amorphous-forming region by sputtering and by melt-quenching methods. Increasing substrate temperature may decrease the quenching rate of the sputtered molecules on the substrate. Increasing sputtering power will increase the thermal energy of the sputtered molecules, thus reduce the quenching rate of the sputtered molecules. Increasing sputtering time gives a similar effect as increasing power or increasing substrate temperature, but the true reason is not certain at the moment. One explanation is that the substrate temperature shifts toward higher temperature as the film grows thick and another explanation is a possible micro-structural change of the sputtered film as the film grows thick. After all, increasing substrate temperature, increasing sputtering power or increasing sputtering time affect the amorphous regions of sputtered films in a similar way as the decreasing cooling rate does for the glass-forming regions by the melt-quenched method.

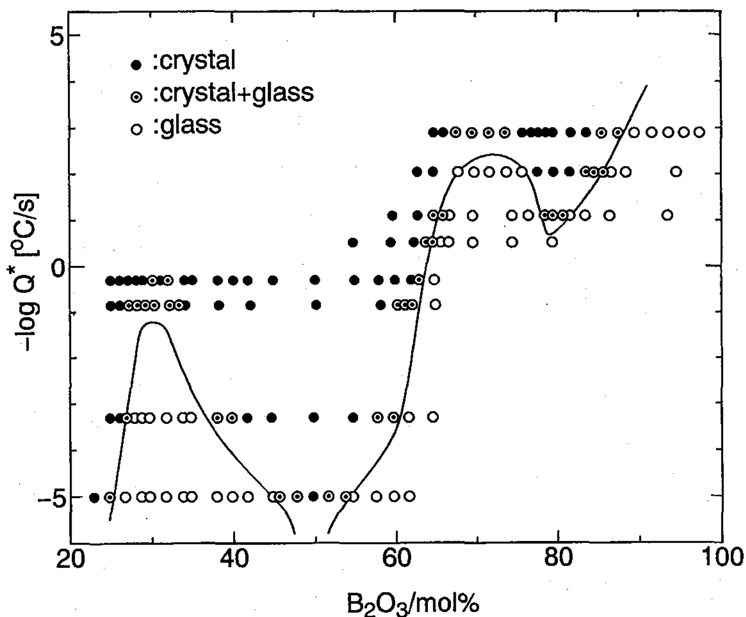

Fig. 9. Glass-forming regions by the melt-quenching method for various cooling rates in the B_2O_3-Na_2O system. The lines indicate the critical cooling rate Q^*.

4. CONCLUSION

The amorphous region in the sputtered films of the B_2O_3-Na_2O system was determined under various sputtering conditions. The compositional range of the amorphous regions was found considerably larger than that of the melt-quenched glasses of the same system. This result

is reasonable if sputtering method is regarded as a modified melt-quenching technique of ultra-high quenching rate. The amorphous regions were reduced with increasing sputtering power, substrate temperature and sputtering time.

ACKNOWLEDGEMENT

The authors express sincere thanks to Prof. Hanada of Kyoto University for his technical support to measure the film thickness of the sputtered films.

REFERENCES

(1) D.R. Secrist and J.D. Mackenzie, "Modern Aspects of the Vitreous State", Vol. 3, ed. J.D. Mackenzie, Butterworth, London, p. 161 (1961).
(2) for instance, T. Hanada, T. Aikawa and N. Soga, *J. Non-Cryst. Solids*, **50**, 397–405 (1982).
(3) R. Ota, Y. Nagoshi and J. Fukunaga, *Zairyo (Japanese)*, **41**, 56–72 (1992).
(4) R. Ota, T. Murakami and J. Fukunaga, *Nihon-Kagaku-Kaishi*, 1386–91 (1991).
(5) C.E. Adams and J.T. Quan, *J. Phys. Chem.*, **70**, 331–40 (1966).
(6) Alfred Buchler and J.B. Berkowitz, *J. Chem. Phys.*, **39**, 286–91 (1963).
(7) Von C. Kroger and L. Sorstrom, *Glastechn. Ber.*, **38**, 313–21 (1965).
(8) R. Ota and N. Soga, *Zairyo*, **30**, 600–606 (1987).
(9) K. Wasa and S. Hyakawa, "Supatta-Gijyutu" (Japanese), Kyoritsu Pub. Co., p. 182 (1988).
(10) R. Ota and N. Soga, *J. Ceram Soc. Japan*, **90**, 531–37 (1982).
(11) R. Ota, T. Kato and N. Soga, *J. Ceram Soc. Japan*, **91**, 73–81 (1983).